Available online at www.sciencedirect.com
ScienceDirect
Journal of the European Ceramic Society 28 (2008) 2191–2197
www.elsevier.com/locate/jeurceramsoc

Mullite/ZrO_2 coatings produced by flame spraying

C. Cano, E. Garcia, A.L. Fernandes, M.I. Osendi, P. Miranzo *

Institute of Ceramics and Glass, CSIC, Madrid, Spain

Received 16 December 2007; received in revised form 20 February 2008; accepted 29 February 2008

Abstract

Mullite/ZrO_2 coatings of the eutectic composition (80/20% (v/v) mullite/ZrO_2) have been flame sprayed on both ceramic and metal substrates. Being as-sprayed coatings mostly amorphous, thermal treatments at temperatures in the range of 1000–1300 °C promote crystallization leading to an increase of the hardness and elastic modulus. By in situ heating of the coatings, using the oxyacetylene torch, uncracked crystallised coatings having good mechanical properties are readily produced. The information supplied by the Al_2O_3–ZrO_2–SiO_2 phase equilibrium diagram provides insight into the complex microstructure observed in the coatings.

Keywords: Flame sprayed coatings; Mullite; ZrO_2; Microstructure; Mechanical properties

1. Introduction

Thermal sprayed ceramic coatings are commonly used for protection of metals and seldom ceramic components against temperature, corrosion and erosion.[1] Among the different thermal spraying methods, flame spraying stands out as a very cost-effective technique. Nevertheless, very little work has been done on flame spraying of ceramic powders. Certainly, this technique can be adequate for ceramic compositions melting at temperatures under 2500 °C as in present work, where a mullite/ZrO_2 mixture was chosen for spraying. The composition 80/20% (v/v) mullite/ZrO_2 was selected because it is very close to the 1750 °C invariant point of the corresponding equilibrium phase diagram,[2] which assures a substantial liquid formation at the thermal spraying temperature.

The feasibility of pure mullite coatings as thermal barriers for metal components in diesel engines and as environmental barriers for SiC-based components in the new generation of turbines has been considered in several works.[3–8] Alternative to these coatings that may show enhanced toughness as happens in bulk composites[9,10] are thermal sprayed mullite/ZrO_2 coatings. Surprisingly, there are few works devoted to these coatings[11–14] and most of them are produced by plasma spraying the Al_2O_3–$ZrSiO_4$ stoichiometric mixture, which ideally reacts to form a composite of mullite (33.4 mol %) and ZrO_2 (66.6 mol %) phases. Just one of these works[14] develops mullite/ZrO_2 materials from mullite/ZrO_2 mixtures but none produces mullite/ZrO_2 coatings by the low-cost thermal flame spraying method.

It should be noticed that thermal spraying of mullite-based compositions generally gives amorphous coatings due to the fast cooling rates that freeze the high temperature phases,[5,6] which can crystallize when annealed at temperatures of ~1000 °C.[6] In the case of mullite/ZrO_2 coatings, the coexistence of amorphous and crystalline phases has been proved by Li and Khor[11] using transmission electron microscopy. These authors observed completely melted splats that coexist with some unmolten particles and ZrO_2 precipitates.

The objective of the present work is to study the viability of flame spraying mullite/ZrO_2 mixtures on both ceramic and metal substrates. Possible thermal treatments promoting crystallization without substantial crack formation and enhancing mechanical response of the coating are also explored. Finally, a deep analysis of the coating microstructures is done and data are discussed in reference to information provided by the Al_2O_3–SiO_2–ZrO_2 phase equilibrium diagram.

* Corresponding author at: Institute of Ceramics and Glass, CSIC, C/ Kelsen 5, Campus de Cantoblanco, 28049 Madrid, Spain.
Tel.: +34 917355872/34 917355840; fax: +34 917355843.
E-mail address: pmiranzo@icv.csic.es (P. Miranzo).

0955-2219/$ – see front matter © 2008 Elsevier Ltd. All rights reserved.
doi:10.1016/j.jeurceramsoc.2008.02.021

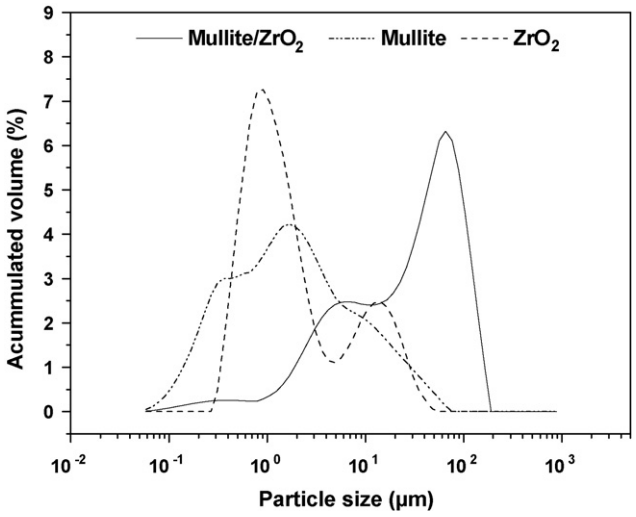

Fig. 1. Particle size distribution for mullite, m-ZrO_2 and the agglomerated mullite/ZrO_2 powders.

2. Experimental

Both AISI 304 L stainless steel and stoneware ceramic plates of 30 mm × 30 mm × 5 mm were used as substrates. Metallic substrates were grit-blasted with corundum particles of 99.60 wt% purity and 0.53 mm of mean particle size, using an air pressure of 0.4 MPa, an incidence angle of ∼45° and a gun-to-substrate distance of 130 mm. Roughness was measured using a profilometer (Perthometer M1. Mahr GMBH. Germany). An average surface roughness of 5.1 ± 0.5 μm and a mean roughness depth of 27.6 ± 2.4 μm were measured for the stainless steel substrates. The ceramic substrates had a roughness of Ra = 2.4 ± 0.2 μm and Rz = 15.8 ± 1.7 μm, and which was, therefore, enough to assure the mechanical anchoring of the coating.

Commercially available mullite ($3Al_2O_3{\cdot}2SiO_2$) (Baikolox SASM. Baikowski Chimie, France) and monoclinic ZrO_2 (SF-EXTRA, Z-Tech Zirconia, US) powders were employed. The corresponding particle size distributions measured by laser diffraction (Mastersizer S, Malvern, UK) are plotted in Fig. 1. The mean particle size for mullite was 1.53 μm, with a distribution width between 0.05 μm and 80 μm. The ZrO_2 particle size spanned from 0.05 μm to 40 μm, with a mean particle size of 1.21 μm.

The mullite/ZrO_2 80/20% (v/v) powder mixture was homogenized and then agglomerated to get the adequate shape and size for thermal spraying. Firstly, the mullite and ZrO_2 mixture was ball milled for 21 h in isopropyl alcohol with nylon balls. Alcoholic media was eliminated in a rotary-evaporator to avoid phase segregation. Then, the mixture was oven dried at 65 °C and sieved through a 100 μm mesh. Secondly, powders were mixed with an organic binder (Paraloid B-67, Rohm and Haas, PA, USA) in acetone. The resulting paste was sieved through a 63 μm mesh rejecting larger particles; next, powders were sieved through a 32 μm mesh to discard smaller particles. This batch of selected sizes was treated at 1600 °C for 1 h to confer particles enough consistency for injection in the spraying system. Powders were maintained in an oven at 120 °C just before spraying to avoid moisture and assure a good flow ability. The thus conditioned mullite/ZrO_2 powders (Fig. 1) showed a multimodal size distribution, with a main peak centred at 65 μm and a wide band due to aggregates under 10 μm, which must correspond to agglomerates smashed in the sieving process. The aggregates were clusters of fine grains (1–2 μm) as clearly seen in the micrograph of Fig. 2.

The powders were flame sprayed onto the substrates using an oxygen-acetylene gun (model CastoDyn DS 8000, Eutectic Castolin, Spain). The torch input power was 28 kW and the powder feed rate was ∼0.6 kg h^{-1}. The acetylene/oxygen volumetric flow ratio was that of the stoichiometric acetylene/oxygen mixture ($\Phi = 1$). The oxygen and acetylene pressures were 4×10^5 and 7×10^4 Pa, respectively. The adiabatic flame temperature calculated for the present experimental conditions was ∼3100 °C.[15] An stand-off distance of 200 mm was selected after some initial proofs at different distances. Mullite powders were also sprayed under the same conditions just for comparative purposes.

Chemical composition of the mullite/ZrO_2 mixture (before and after conditioning) as well as of the sprayed coating after

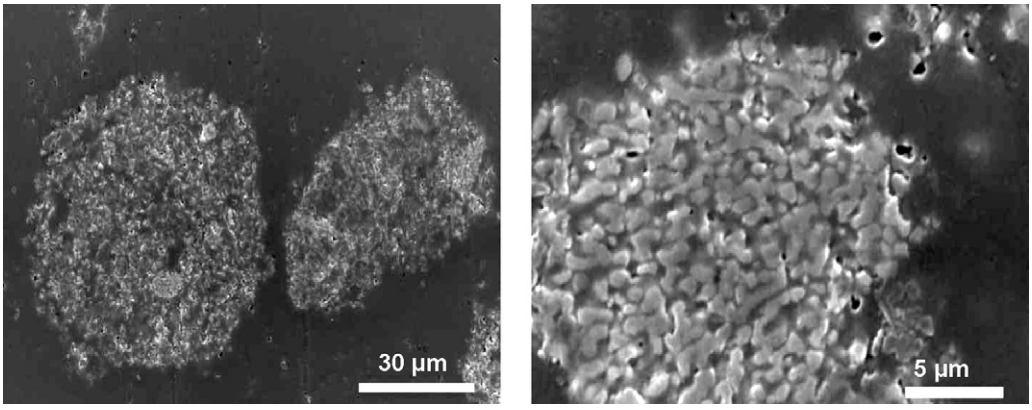

Fig. 2. SEM micrographs of cross sectioned aggregates of mullite/ZrO_2. Secondary electron (SE) image.

comminution was determined using energy dispersive X-ray fluorescence methods (ED-XRF, Philips, model PW-2424, The Netherlands) in order to evaluate possible contaminations and/or SiO_2 volatilization during spraying.

Differential thermal analysis (DTA, STA 409, Netzsch, Germany) was done on the crushed coatings for studying phase changes up to 1500 °C. Then different thermal treatments were selected to promote crystallization, which were carried out on coatings deposited over the ceramic substrates. Alternatively, an in situ heating was also tried using the torch as heating source. The sprayed coatings were heated until red glow was observed on the surface (900 – 1000 °C).

The microstructure of the different coatings was analyzed on polished cross sections and on top surfaces using a field emission scanning electron microscope (SEM, HITACHI S-4700, Japan). Phase compositions were calculated from energy dispersive X-ray spectroscopy (EDS) standardless point analyses, using Proza $\varphi(\rho z)$ corrections. Crystalline phases in the coatings were identified by X-ray diffraction analysis (XRD – Siemens D5000, Germany). Hardness was measured by Vickers indentation tests done on the coating cross sections. At least 5 measurements at a load of 2.9 N for 15 s were completed for each coating using a hardness testing machine (ZHU 2,5; Zwick GmbH & Co. KG, Germany) that simultaneously recorded load and specimen displacement. From load displacement curve during the unloading cycle the equipment software calculates the elastic modulus of the specimen. Besides, additional Vickers indentation tests[16] with a load of 19.6 N were done for toughness evaluation of the in situ treated coatings, as well-developed indentation cracks formed in this coating.

Table 1
ED-XRF chemical compositions of the initial mullite/ZrO_2 mixture, the agglomerated powders and the powdered sprayed coating

(wt%)	Mullite/ZrO_2 original	Mullite/ZrO_2 after conditioning	Mullite/ZrO_2 coating
Al_2O_3	46.1	45.6	47.6
SiO_2	17.6	17.9	14.4
ZrO_2	35.4	35.5	36.6
Fe_2O_3	0.026	0.059	0.052
P_2O_5	0.035	0.037	0.042
CaO	0.019	0.037	0.047
TiO_2	0.028	0.022	0.023
Cr_2O_3	0.008	0.008	0.010
Na_2O	0.078	0.088	0.045
HfO_2	0.75	0.72	0.75
K_2O	–	0.001	–
Y_2O_3	0.20	0.14	0.19
SO_3	0.089	0.095	0.060

3. Results and discussion

Data provided by ED-XRF analysis of the starting powder mixture, the conditioned powders and the coatings, are collected in Table 1. Neither the $SiO_2/Al_2O_3/ZrO_2$ ratio nor the impurity content was affected by the agglomeration process. Furthermore, spraying had no significant effect over the impurity content, but the relative SiO_2 content decreased about 20% in the coating, thus inferring some SiO_2 volatilization due to the high process temperatures and the reducing conditions in some zones of the combustion flame.[17] A similar effect was also observed in mullite glasses produced by quenching plasma sprayed melts.[18]

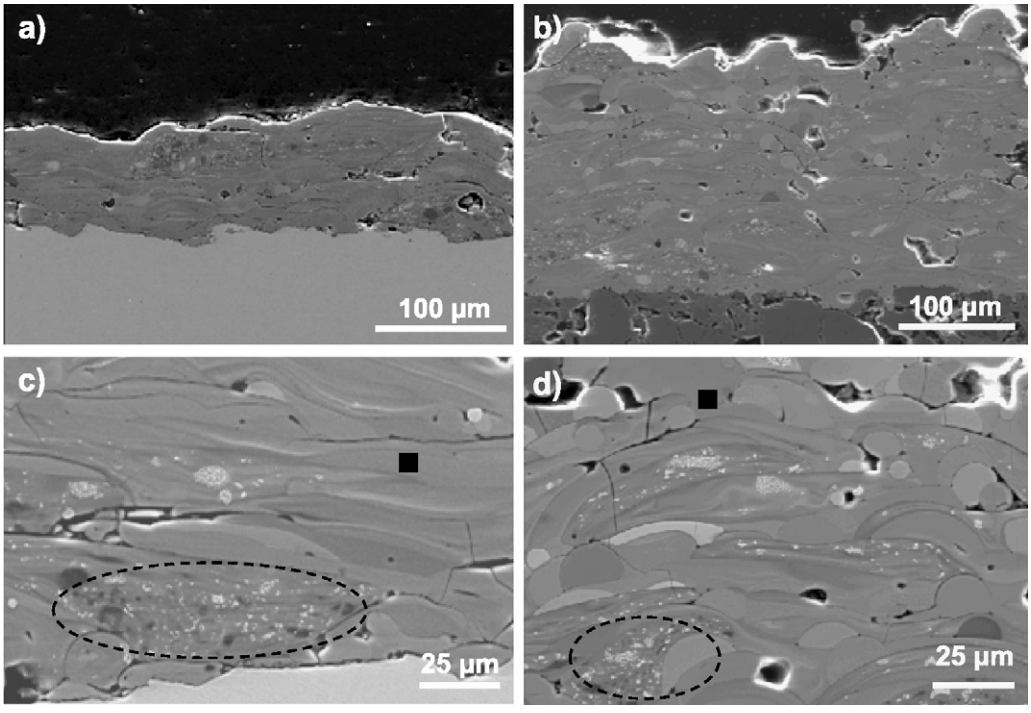

Fig. 3. SEM micrographs (SE images) of the cross sections of the coatings deposited onto stainless steel (a) and (c), and stoneware (b) and (d). The ■ symbol points the major smooth splats and dashed ellipse points some partially molten splats.

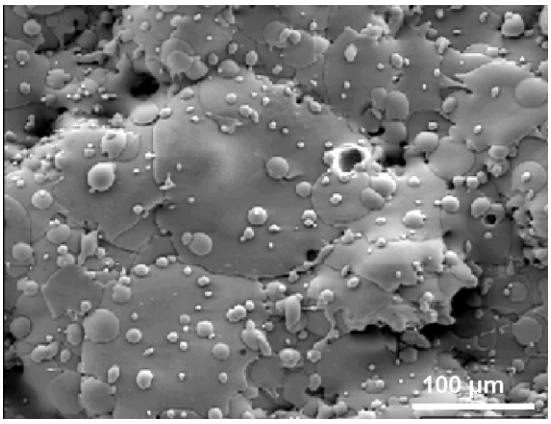

Fig. 4. SEM micrograph (SE image) of the top surface of the coating flame sprayed on stainless steel.

Thickness was about 100 μm for the coating flame sprayed onto the stainless steel (Fig. 3a), showing big disk-shaped splats when observing the top surface (Fig. 4). Interfacial reactions between the coating and the metallic substrate were not detected indicating a pure mechanical anchorage. Some inter-splats and interfacial cracks were clearly observed in this coating (Fig. 3c).

The mullite/ZrO_2 coating sprayed onto the ceramic substrate (Fig. 3b) had thickness of 300 μm and showed better bonding between splats (Fig. 3d) and also between the coating and the substrate as compared to similar coating over the stainless steel substrate. This can be associated to two effects; first, the closer thermal expansion coefficients of the stoneware ceramics to the coating and, second, the slower cooling rate of this system due to the lower thermal conductivity of the stoneware (1.5 W/m K).[19]

XRD patterns of the as-sprayed coatings were similar for both substrate systems (Fig. 5) showing an amorphous background with overlaid peaks corresponding to crystalline phases identified as mullite, m-ZrO_2 and t-ZrO_2. The formation of the t-ZrO_2 polymorph may be explained by both the small size of the precipitates and their confinement in the matrix, which generates compressive stresses in the particle at cooling.[20]

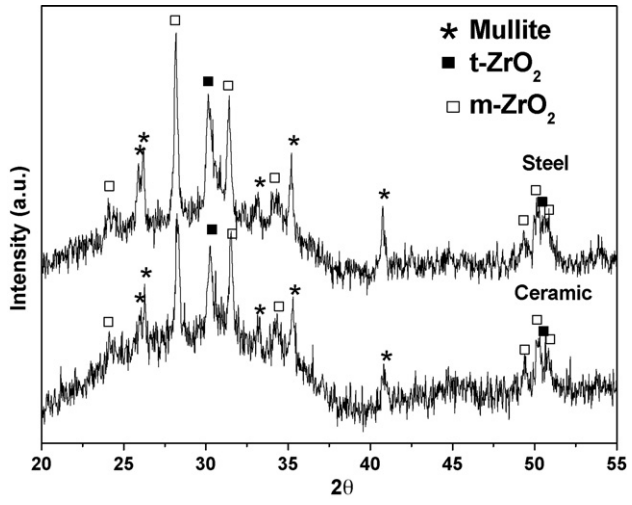

Fig. 5. XRD patterns of the as-sprayed coatings deposited on steel and ceramic substrates.

Most of the splats in the coatings (marked with ■ in Fig. 3 c and d) were formed by a continuous phase with EDS compositions having Al_2O_3/SiO_2 ratios similar to that of mullite (2.55 in wt%) and ZrO_2 contents ranging from 20 to 60 wt%. In addition to these predominant smooth splats, Fig. 3 also shows the presence of some splats containing dark and bright phases. These dark phases (▲ in Fig. 6a) always had compositions close to that of mullite and they may correspond to either unmolten mullite grains or mullite crystals grown from the liquid phase

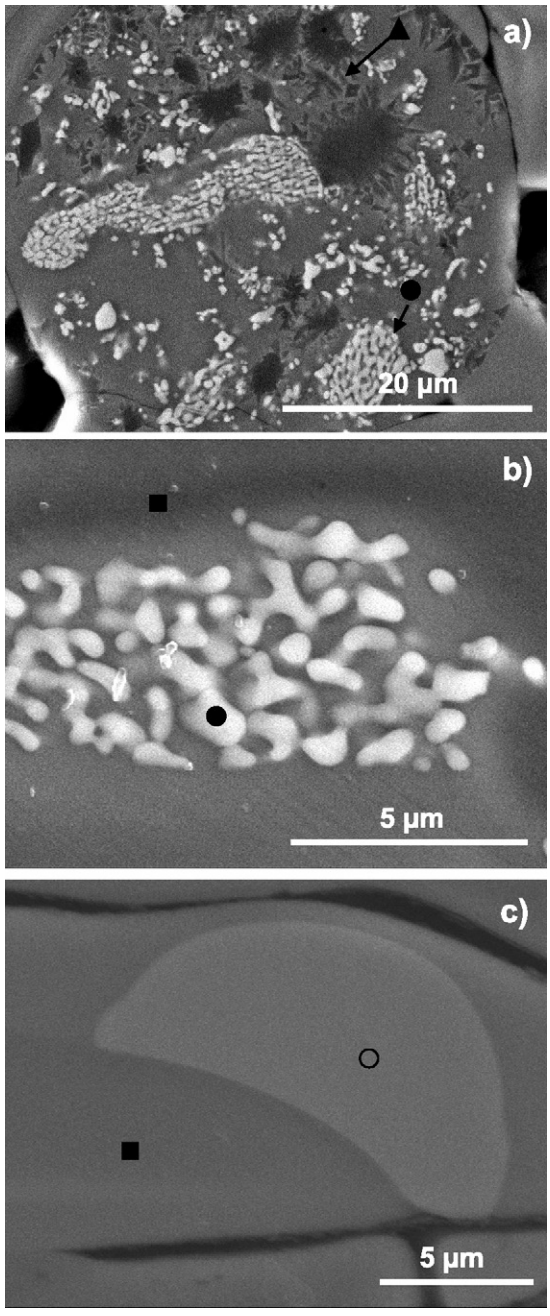

Fig. 6. SEM micrographs (SE images) of the cross section of the coating sprayed on stainless steel showing details of the microstructure: (a) a partially crystallized splat, (b) higher magnification of some ZrO_2 crystallizations and (c) phase with ZrO_2–Al_2O_3 rich composition (■, smooth splats; ▲, mullite; ●, ZrO_2 and ○, ZrO_2–Al_2O_3).

during cooling. On the other hand, EDS compositions of the round bright precipitates (● in Fig. 6a and b) were difficult to estimate due to their small sizes (<1 μm) but, as they were ZrO_2-enriched (>95 wt%), they should correspond to the ZrO_2 phase detected by XRD. Finally, other clear phases (◯ in Fig. 6c) of larger sizes (5–10 μm) that had SiO_2 content below 10 wt% and ZrO_2 contents ranging from 90 to 40 wt% were detected. In some cases, the SiO_2 loss was so high that this metastable phase even showed compositions within the ZrO_2–Al_2O_3 binary system. It should be pointed out that data provided by chemical analysis (Table 1) gives only the average SiO_2 volatilization and what really happens is a local phenomenon, which depends on the temperature reached by the flying aggregates and, therefore, on their downstream location.[17]

Compositions for each one of these phases were located in the Al_2O_3–SiO_2–ZrO_2 equilibrium phase diagram,[2,21] as presented in Fig. 7 together with the chemical analysis of the powdered coating obtained by ED-XRF (⊗ in that figure). All of the major smooth splats had compositions located just at the mullite–ZrO_2 tie-line, close to the average coating composition (ED-XRF data), then they correspond to metastable amorphous phases that would crystallize on cooling in mullite and ZrO_2. The clear phases of large size detected in the coatings having SiO_2 poorer compositions are located in the left side of the ternary equilibrium phase diagram (◯ in Fig. 7) with $Al_2O_3/ZrO_2/SiO_2$ ratios far from the mullite–ZrO_2 tie-line. Those areas would also be metastable amorphous phases that should crystallize under slow cooling rates in ZrO_2 and Al_2O_3. Therefore, flying aggregates had enough time at high temperature to get complete melting and, due to the rapid solidification process, formed homogeneous splats of amorphous metastable phases with compositions depending on the reached temperature. However, some splats were not homogeneous in composition showing submicronic phases associated to ZrO_2 and mullite crystals. These may correspond to either flying aggregates from the coolest area of the torch that did not

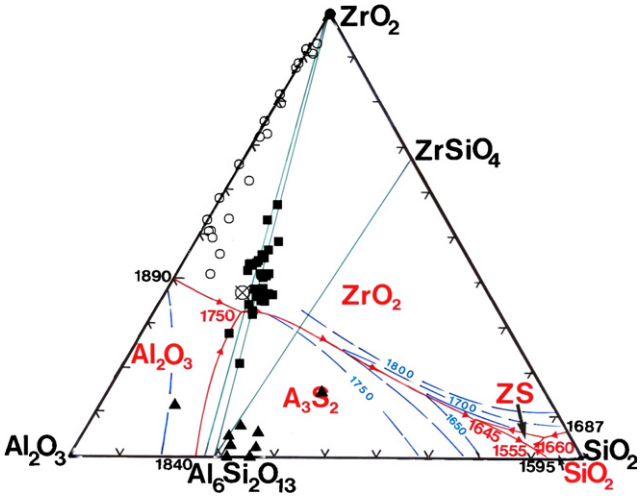

Fig. 7. Al_2O_3–SiO_2–ZrO_2 equilibrium phase diagram[2] showing points corresponding to the EDS compositions of the different phases found throughout the coatings (■, smooth splats; ▲, mullite; ●, ZrO_2; ◯, ZrO_2–Al_2O_3 and ⊗, the ED-XRF analysis of the coating).

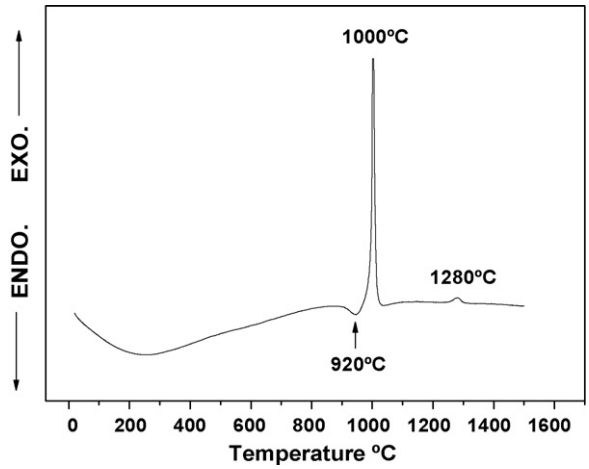

Fig. 8. DTA of the powdered as-sprayed coating done on stainless steel.

get complete melting or partially crystallized molten droplets that cooled down during flying below the eutectic point of the Al_2O_3–SiO_2–ZrO_2 system.

DTA of the powdered coating showed two exothermic peaks at ∼1000 °C and ∼1280 °C (Fig. 8), both associated to mullite crystallization from a Al_2O_3/SiO_2 mixture according to data from the literature.[22,23] The first peak corresponds to the formation of an Al–Si spinel and the simultaneous crystallization of t-ZrO_2 from the amorphous material, whereas the second peak matches with the spinel to mullite transformation and growth. The small endothermic peak found at 920 °C may be associated to the activation energy for crystallization. Considering these data, the whole assembly was heated at temperatures of 1000 and 1300 °C for 1 h in a furnace. As shown in Fig. 9a, comparing with the XRD pattern of the mainly amorphous as-sprayed coating (Fig. 5), the coating treated at 1000 °C showed strong peaks of t-ZrO_2 and traces of mullite, m-ZrO_2 and spinel, although the width of the peaks indicated very small crystallite sizes. At 1300 °C, t-ZrO_2 and mullite peaks became narrower and better defined inferring a grain growth process. The XRD pattern of the in situ treated coating (Fig. 9b) also shows the presence of mullite, t- and m-ZrO_2.

As seen in Fig. 10, some cracks grew during the heating/cooling post-treatments, which may be due to volume changes upon crystallization.[6] A higher magnification view of the coating treated at 1300 °C shows typical dendrite crystals of ZrO_2 phase (Fig. 10b). Crack formation was avoided when coating alone was subjected at high temperature (in situ heating) as observed in Fig. 11a. The crack suppression in this coating can be explained because matrix was still at high temperature during the in situ heat treatment and may accommodate volume changes associated to crystallization. This coating had a very fine microstructure showing many mullite and ZrO_2 nuclei within the splats. Additionally, dendrite growth of ZrO_2 crystals from the matrix (Fig. 11b) and ZrO_2 nuclei inside the ZrO_2–Al_2O_3 phases (Fig. 11c) were observed.

Hardness and elastic modulus of the as-sprayed and heat treated mullite/ZrO_2 coatings are given in Fig. 12. The mullite coating, prepared as a reference, showed hardness of 6.6 GPa and

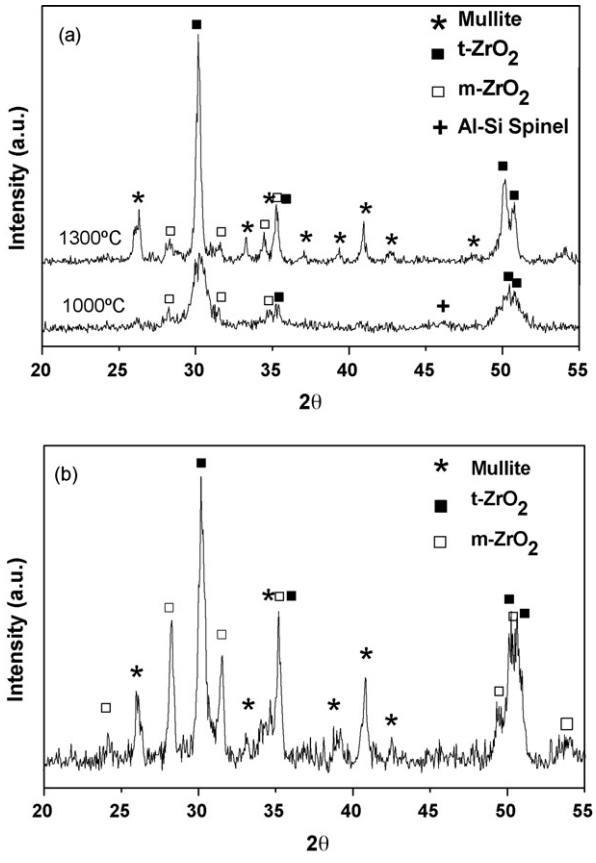

Fig. 9. XRD patterns of the treated mullite/ZrO_2 coatings: (a) furnace treatment at 1000 and 1300 °C and (b) in situ treatment.

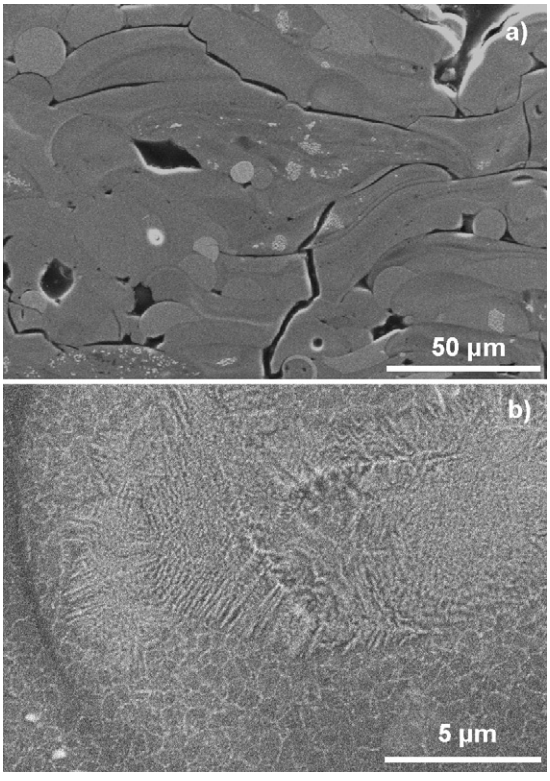

Fig. 10. SEM micrographs (SE images) of the coating treated at 1300 °C showing (a) the general microstructure and (b) a detail of ZrO_2 dendrite growth.

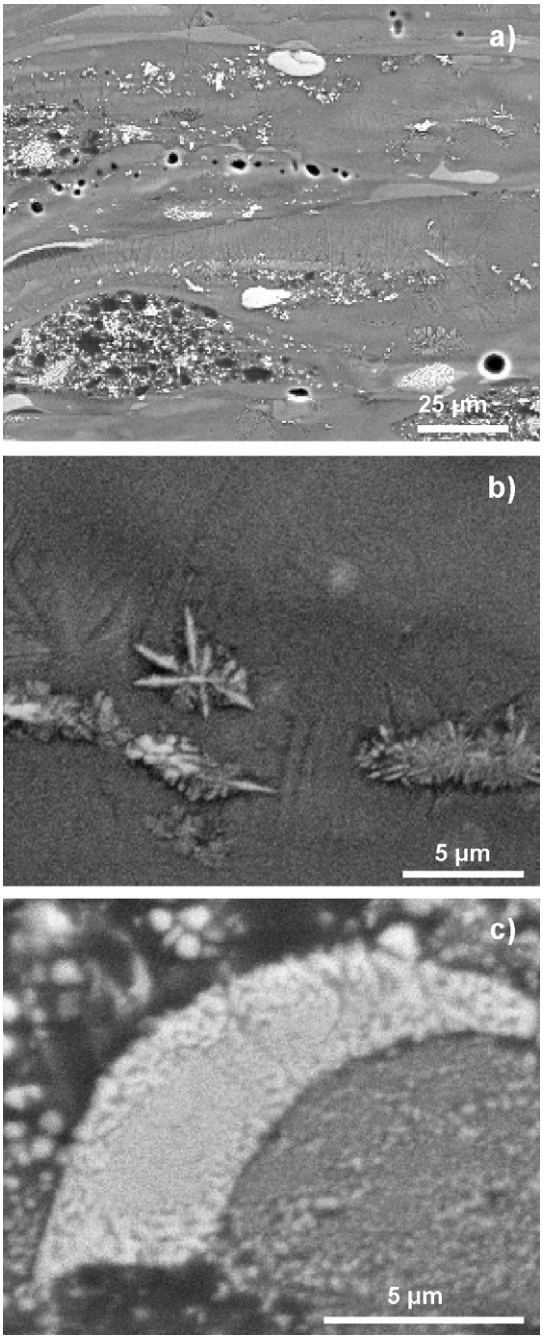

Fig. 11. Different magnification SEM micrographs (SE images) of the in situ treated coating: (a) general view, (b) dendrite growth of ZrO_2 crystals from the matrix and (c) ZrO_2 crystallizations inside the ZrO_2–Al_2O_3 amorphous phases.

elastic modulus of 61 GPa, the later being similar to that reported elsewhere.[5] By adding ZrO_2, hardness and elastic modulus increased up to 8.5 and 126 GPa, respectively, values significantly higher than those reported till now.[12] These parameters further increased with the extent of crystallization in the coatings reaching maximum values of 14 GPa (H) and 180 GPa (E) for both the 1300 °C and the in situ treated coatings. These values are close to those reported for similar bulk mullite/ZrO_2 composites.[9] Toughness was measured for the in situ treated coating as well-developed indentation cracks occurred in this

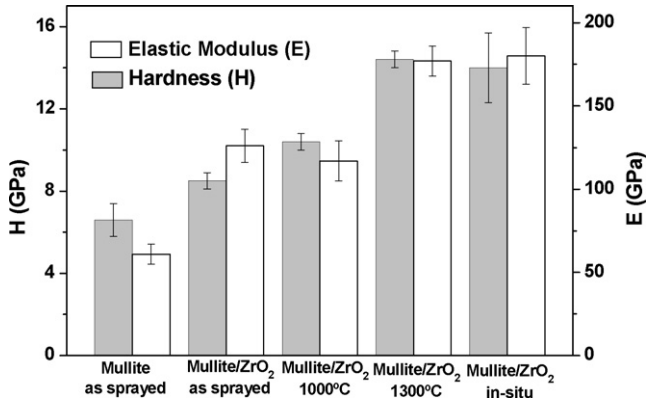

Fig. 12. Hardness and elastic modulus of the as-sprayed and heat treated coatings.

case, reaching values of 2 MPa $m^{1/2}$, similar to the figures of plasma sprayed mullite/ZrO_2 coatings.[12]

4. Conclusions

For the first time, mullite/ZrO_2 coatings have been flame sprayed on both metal and ceramic substrates. The as-sprayed coatings were mostly amorphous but thermal treatments at temperatures in the range of 1000–1300 °C improved their crystallinity, enhancing their hardness and elastic modulus. The development of cracks during the thermal treatments can be avoided by the in situ heating using the flame torch. This treatment favoured crystallization in the coatings, leading to mechanical properties well above those, reported for these kinds of coatings obtained by plasma spraying.

The major amorphous splats forming the coatings had compositions in the mullite–ZrO_2 tie-line, but some shifted from the original composition due to local SiO_2 volatilization because of the very high temperatures developed and the combustion atmospheres. Some partially crystallized splats were also detected probably associated to aggregates flying at lower temperatures.

Acknowledgments

This work was supported by MEC (Ministry of Education and Science, Spain), MAT 2003-06147-C04-01 and MAT2006-07118. Thanks are given to S. de Aza and F.J. Valle for helping in the equilibrium phase diagram discussion and in the ED-XRF analyses, respectively.

References

1. Padture, N. P., Gell, M. and Jordan, E. H., Thermal barrier coatings for gas-turbine engine applications. *Science*, 2002, **296**, 280–284.
2. Pena, P. and De Aza, S., The zircon thermal behaviour: effect of impurities. *J. Mater. Sci.*, 1984, **19**, 135–142.
3. Ramaswamy, P., Seetharamu, S., Varma, K. B. R., Raman, N. and Rao, K. J., Thermo-mechanical fatigue characterization of zirconia (8%Y_2O_3–ZrO_2) and mullite thermal barrier coatings on diesel engine components: effect of coatings on engine performance. In *In Proceedings of the Institution of Mechanical Engineers*, 2000, pp. 729–742.
4. Ramaswamy, P., Seetharamu, S., Varma, K. B. R. and Rao, K. J., Thermal shock characteristics of plasma sprayed mullite coatings. *J. Therm. Spray Technol.*, 1987, **7**, 497–504.
5. Rohan, P., Neufuss, K., Matejicek, J., Dubsky, J., Prchlik, L. and Holzgartner, C., Thermal and mechanical properties of cordierite, mullite, and steatite produced by plasma spraying. *Ceram. Int.*, 2004, **30**, 597–603.
6. Lee, K. N., Miller, R. A. and Jacobson, N. S., New generation of plasma-sprayed mullite coatings on silicon carbide. *J. Am. Ceram. Soc.*, 1995, **78**, 705–710.
7. Lee, K. N., Fox, K. N. D. S., Eldridge, J. I., Zhu, D. M., Robinson, R. C., Bansal, N. P. *et al.*, Upper temperature limit of environmental barrier coatings based on mullite and BSAS. *J. Am. Ceram. Soc.*, 2003, **86**, 1299–1306.
8. Belmonte, M., Advanced ceramic materials for high temperature applications. *Adv. Eng. Mater.*, 2006, **8**, 693–703.
9. Scheneider, H. and Komarneni, S., *Mullite*. Wiley-VCH Verlag GmbH & Co., KgaA, Weinheim, Germany, 2005.
10. Moya, J. S. and Osendi, M. I., Microstructure and mechanical properties of mullite/ZrO_2 composites. *J. Mater. Sci.*, 1984, **19**, 2909–2914.
11. Li, Y. and Khor, K. A., Microstructure and composition analysis in plasma sprayed coatings of Al_2O_3/$ZrSiO_4$ mixtures. *Surf. Coat. Tech.*, 2002, **150**, 125–132.
12. Li, Y. and Khor, K. A., Mechanical properties of the plasma-sprayed Al_2O_3/$ZrSiO_4$ coatings surf. *Coat. Tech.*, 2002, **150**, 143–150.
13. Das, S., Ghosh, S., Pandit, A., Banyopadhyay, T. K., Chattopadhyay, A. B. and Das, K., Processing and characterization of plasma sprayed zirconia-alumina-mullite composite coating on a mild-steel substrate. *J. Mater. Sci.*, 2005, **40**, 5087–5089.
14. Chang, K., Rezaie, H. R., Alexander, I. C., Davies, H. A., Messer, P. F. and James, P. F., Preparation of zirconia mullite flakes via a plasma rapid solidification process using starting materials derived from a sol-gel technique. *J. Non-Cryst. Solids*, 2001, **290**, 231–244.
15. Cano, C., Belmonte, M., Osendi, M. I. and Miranzo, P., Effect of the type of flame on the microstructure of $CaZrO_3$ combustion flame sprayed coatings. *Surf. Coat. Technol.*, 2007, **201**, 3307–3313.
16. Miranzo, P. and Moya, J. S., Elastic plastic indentation in ceramics: a fracture toughness determination method. *Ceram. Int.*, 1984, **10**, 147–152.
17. Ozturk, A. and Cetegen, B. M., Modeling of precipitate formation in precursor droplets injected axially into an oxygen/acetylene combustion flame. *Mater. Sci. Eng. A*, 2006, **422**, 163–175.
18. Schmucker, M., Schneider, H., Poorteman, M., Cambier, F. and Meinhold, R., Constitution of mullite glasses produced by ultra-rapid quenching of plasma-sprayed melts. *J. Eur. Ceram. Soc.*, 1995, **15**, 1201–1205.
19. Pablos, A., Miranzo, P. and Osendi, M.I., Thermal conductivity of different materials used in buildings. unpublished data.
20. Heuer, A. H., Claussen, N., Kriven, W. M. and Rühle, M., Stability of tetragonal ZrO_2 particles in ceramic matrices. *J. Am. Ceram. Soc.*, 1982, **65**, 642–650.
21. Qureshi, M. H. and Brett, N. H., Phase equilibria in ternary systems containing zirconia and silica. 2. System Al_2O_3–ZrO_2–SiO_2. *Trans. British. Ceram. Soc.*, 1968, **67**, 569–572.
22. Srikrishna, K., Thomas, G., Martinez, R., Corral, M. P., De Aza, S. and Moya, J. S., Kaolinite-mullite reaction series: a TEM study. *J. Mater. Sci.*, 1990, **25**, 607–612.
23. Tkalcec, E., Kurajica, S. and Ivankovic, H., Diphasic aluminosilicate gels with two stage mullitization in temperature range of 1200–1300 °C. *J. Eur. Ceram. Soc.*, 2005, **25**, 613–626.